Understanding the Factors Influencing Carbon Dioxide Dilution in an Aluminum Electrolysis Cell

Mohammadreza Basohbatnovinzad[1], Lukas Dion[2], Kadiata Ba[3], Simon-Olivier Tremblay[4], Sébastien Guérard[5] and Jean-François Bilodeau[6]
1. PhD Student
2. Professor University, Director
3. Professor University, Co-Director
4. Research Professionnal
Université du Québec à Chicoutimi, CURAL-GRIPS, Saguenay, Canada
5. Research Scientist, R&D
6. Principal Advisor, R&D
Rio Tinto – Arvida Research and Development Centre, Saguenay, Canada
Corresponding author: mbasohbatn@etu.uqac.ca
https://doi.org/10.71659/icsoba2024-al034

Abstract

The Hall-Héroult process is widely employed worldwide to produce aluminum. Inherently, this process also generates significant emissions of carbon dioxide, a greenhouse gas as a by-product of the reaction. As the bubbles formed during the electrolysis escape from the electrolysis cells, they induce the generation of a gas flow underneath the anodes, which are expelled due to the buoyancy forces of the melt. The rate of the gas flow generated, and the incident gas concentration of the output gas will be dependent on numerous different factors. In this work, a numerical model was developed to replicate the chemical reactions in the vicinity of an anode assembly leading to the generation of carbon monoxide and carbon dioxide. The output gases are then rooted to the gas exaust with fluctuating concentrations due to changes in the conditions, which may result in variations in the amount of carbon dioxide and carbon monoxide being produced under steady state. Hence, the purpose of the experimental plan is to simulate the operations of a specific number of different situations so as to illustrate the extent of the operational conditions that can be expected in the industry in the future. In order to accomplish this purpose, the numerical model was developed using ANSYS Fluent and a validation process was developed to confirm the accuracy of the model. During the investigations, various conditions were meticulously examined, analyzed and evaluated, including the pressure at the gas exhaust point, the air entering the electrolysis process, the effect of current efficiency, the amount of current flowing through the cell, the height of the channel, the anode size and other factors, in order to comprehensively understand the effect of these factors on the concentration of gas within the cell.

Keywords: Hall-Héroult process, Chemical reactions, ANSYS Fluent, Gas concentration, Current efficiency.

1. Introduction

Aluminum is a metal widely used in a variety of applications, including transportation and construction, due to its unique properties [1]. Canada is one of the major producers and exporters of aluminum. In 2020, Canada produced approximately 3.2 million tonnes of aluminum, with 90 % of this production taking place in Quebec [2]. Various strategies, such as increasing energy and material efficiency and incorporating renewable energy sources, have been implemented to reduce the environmental impact of aluminum production. While progress has been made, there is still a long way to go in achieving sustainable aluminum production. The industry must focus on working towards a low-carbon future that balances environmental concerns with economic growth [3].

This project will provide important information regarding the potential CO_2 concentration that can be achieved in an electrolysis cell while also describing the gas properties in terms of chemistry and temperature. This information will help define the applicability of different potential solutions for subsequent CO_2 capture. The level of greenhouse gases in the atmosphere has rapidly risen since the aluminum industrial revolution. The principal gases associated with climate change are carbon dioxide and carbon monoxide. Carbon dioxide is considered the main greenhouse gas due to the significant amount of emissions released into the atmosphere [4]. The aluminum industry is responsible for significant carbon dioxide emissions, as it is the main gas emitted from the electrolysis cells due to the raw materials (petroleum coke and coal tar pitch) used in anode production. The intensity of these gas emissions depends on a multitude of factors such as the current efficiency (ε), cell amperage (I), the electrolysis cell structure, and the anode conditions, namely its ability to withstand O_2 and CO_2 oxidation. Efforts are being made on different levels to reduce GHG emissions, and this study investigates the behavior affecting CO_2 concentration specifically [5]. In this research, a three-dimensional model was created and solved using a numerical method employing a finite difference algorithm within the Ansys/Fluent software. The main objective is to investigate the distribution of gas pressure and CO_2 concentration in the space volume above the crust, under steady-state conditions for a specific set of operating conditions. The proposition of a pathway for potential CO_2 reduction is directly aligned with the main goals of this project. Using the numerical simulations developed, it will be possible to recommend alternative scenarios in which the dilution rate of carbon dioxide can be reduced while limiting the impact on fugitive emissions. The primary indicators examined for validation of the model encompass gas output velocity and concentrations, which are compared with industrial data obtained from previously documented sources in the literature. Additionally, gas collection efficiency is examined in relation to the structure of the gas gathering system and the operation of the electrolytic cell.

2. Literature Review

Many authors have studied the exhaust gas gathering efficiency and CO_2 capture simulation of aluminum electrolysis cells using numerical simulations and Computational Fluid Dynamics software. The Hall-Héroult process, while essential for aluminum production, emits a significant amount of CO_2 into the atmosphere. To address this issue and reduce CO_2 emissions from aluminum production, it is crucial to develop technologies for capturing and storing the CO_2 emitted during the process [6]. Simulation models are created using software like Aspen Plus and Aspen Hysys to evaluate CO_2 capture in aluminum production. In Aspen Hysys, a closed-loop model is used to simulate the CO_2 capture process, which is vital for addressing climate change concerns. These models allow for the analysis of different CO_2 concentrations and capture rates [7]. This research has provided valuable information on potential CO_2 concentrations achievable in electrolysis cells, as well as describe gas properties in terms of chemistry and temperature to define the applicability of potential CO_2 capture solutions. The proposal of a pathway for potential CO_2 reduction aligns directly with the main goals of this project. The aim of this investigation is to evaluate the potential for CO_2 capture from aluminum production by looking at conditions were the CO_2 concentration would be higher than 4 vol% [8].

CFD software is used to implement simulations of a 400 kA aluminum cell. Cell gas collection systems are studied, and the multi-physics field model for the aluminum electrolysis gas gathering system is established. The main conclusions are as follows: The cell has two short sides, called the tap end and the duct end. opening the tapping end side hooding panels has a greater impact on exhaust gas flow than opening the duct end side hooding panels. Due to this, the average flow rate in the two ducts declines and affects the exhaust gas flow rate, indicating that opening the cell hooding panels has little effect, and maintains gas stability under the hood of the electrolysis

cell better [9]. Computational Fluid Dynamics (CFD) software has been used to examine the efficiency of exhaust gas gathering from aluminum electrolysis cells. These simulations focus on managing pollutant levels, such as CO_2 and HF, from aluminum electrolysis plants to maintain or improve air quality. Pressure at the gas exhaust point plays a significant role in reducing gas concentration. Negative pressure in the cell superstructure causes gas to be sucked into the electrolysis hoods. Research also investigates the structure of channel hooding and the efficiency of gas collection based on the gas gathering system and electrolytic cell operating conditions [10].

Efforts will be made in this research to improve or maintain the hooding and gas collection efficiency, as well as suggesting a pathway for easier carbon capture of the CO_2. Several variables are likely to have an influence on gas collection efficiency, including the gas exhaust flow rate, pressure inside the superstructure, and hooding efficiency, which will be explored in this paper and the subsequent steps of this research. In this research, at least one contact reactor is claimed, in which the effluent gas is brought into contact with alumina, and a dust removal device, in which at least some of the alumina has adsorbed pollution from the effluent gas [11].

3. Methodology

In this study, ANSYS-FLUENT was used to replicate half of an AP60 aluminum electrolysis cell. Once reproduced, the model meshing properties were selected in order to minimize the calculation power of the model, while making sure that the selected mesh size is insignificant on the resulting output. Following these changes, the initial boundary layers for a base case scenario were selected and the model was validated using the stoichiometric balance of the model in comparison with literature or reported industrial data. Finally, by changing the boundary layers and shape geometry corresponding to 9 specific cases, a L9 Taguchi design was used to study the effect of 4 parameters on three levels and the results of this sensitivity analysis are presented and discussed. In this article, numerical simulations were developed to evaluate the changing CO_2 concentration trend coming out from the feeder holes, as well as investigating the flowrate distributions from the hooding slits in order to assess the fugitive emission risk.

3.1 The Geometrical Model

There are several elements considered in this model, including the anodes assembly, feeder holes, the inlet airflows in electrolysis, and the channel hooding. The main outlet gas is placed at the end of the channel hooding. A schematic diagram of the computational domain and boundary conditions in the present study is shown in Figure 1. This diagram includes the gas produced by the chemical and electrolysis reactions entering through the feeder holes along with ambient air entering the electrolysis cell from the gap hooding (slits), and all the gas exhaust from the channel hooding at the end of the analysis. To provide spatial information regarding the detailed investigation related to the fugitive gas emission, the slits from the cell are divided into nine regions. Region 1 being closer to the tapping end and region 9 being closer to the duct end.

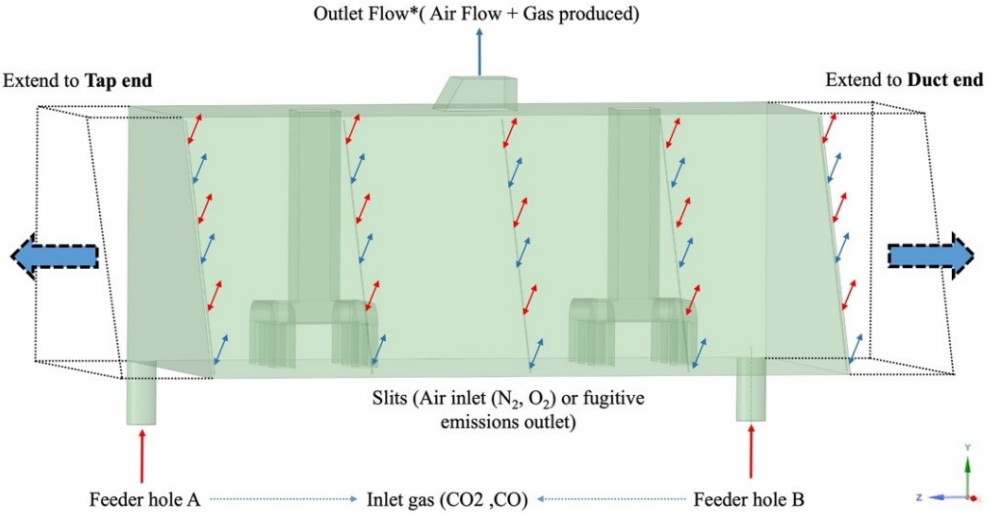

Figure 1. System: Partial section of the cell considered in this work with the inlets and outlets. *The exhausts channels are included in the simulations but not represented for confidential reasons.

3.2 Mesh Analyzing

To perform a mesh analysis, it was necessary to focus on mesh independence as well as mesh quality. As part of the investigation, mesh independence was examined for various elements of the cell, with CO_2 concentration and velocity at the outlet being analyzed. The number of elements selected was based on the verification of the results. As shown in Figure 2, increasing the number of elements led to a decrease in CO_2 concentration and increase in the velocity resulting in results that are more accurate. All results presented in this paper were obtained using 5 300 000 elements. The elements are polyhexagonal in shape, with an element size of 3 mm as shown in Figure 3.

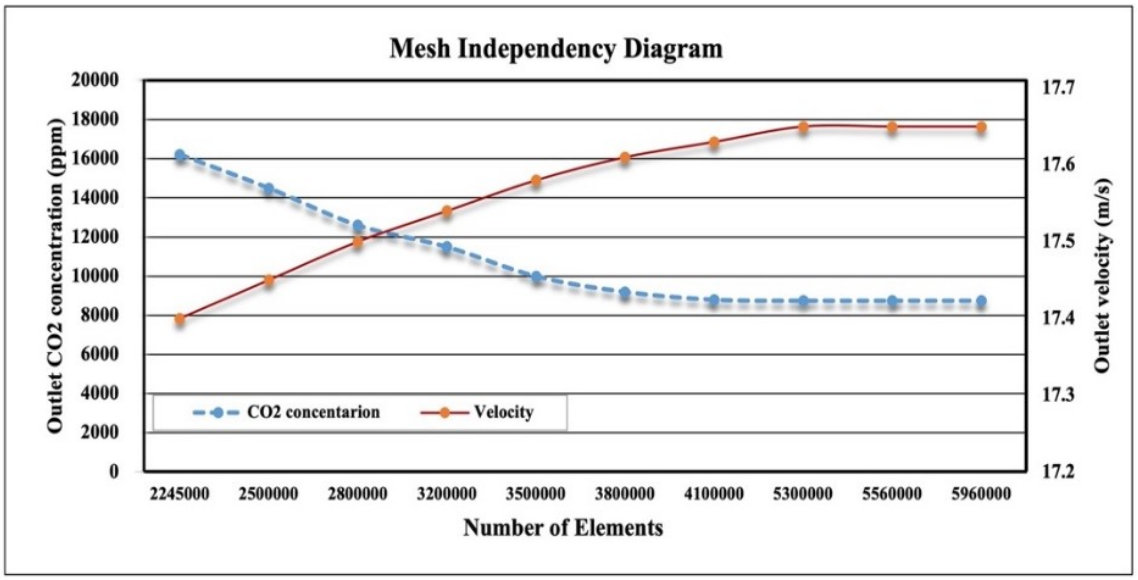

Figure 2. Mesh independency diagram.

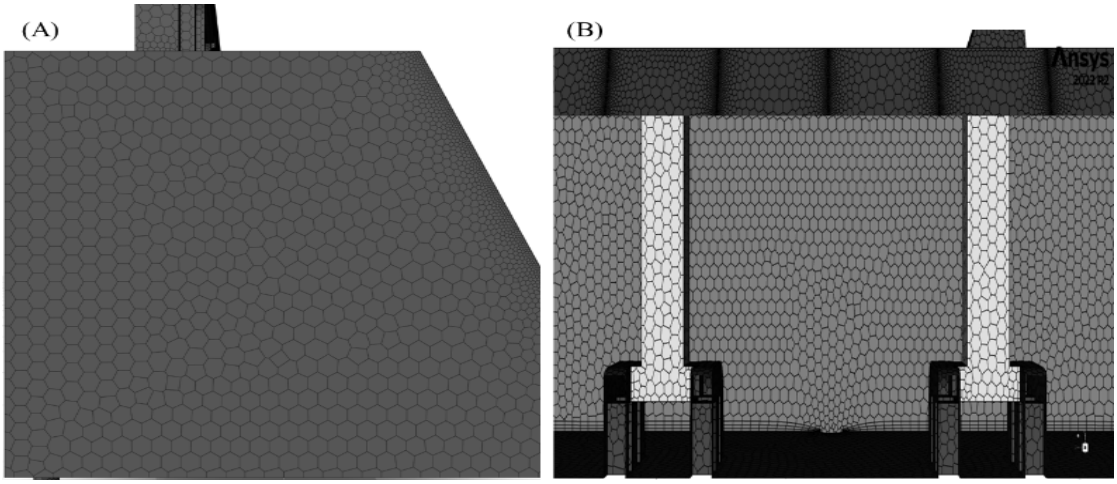

Figure 3. Mesh Used. Left: (A) Side view, Right: (B) Front view.

A high-quality mesh is another important aspect that must be considered to ensure the reliability of predictions. It is defined by maximum skewness, minimum orthogonality, and aspect ratio. The maximum skewness, suggested to be less than 0.85, is 0.65. The orthogonality is 0.92, which exceeds the minimum suggested value of 0.5.

3.3 The Mathematical Model

The model is based on species transport model. Each of the existing phases, i.e., continuous phase includes gas anode produces mixture of air. The continuity equation and the momentum equations are fundamental equations used to describe the behavior of fluid flow. These equations are part of the Navier-Stokes equations, which govern the motion of fluid substances. The continuity and momentum equations are shown in Equation (1) and (2), respectively.

$$\frac{\partial \rho}{\partial t} + \nabla.(\rho \vec{u}) = 0 \tag{1}$$

$$\frac{\partial (\rho \vec{u})}{\partial t} + \nabla.(\rho \overrightarrow{uu}) = -\nabla p + \nabla.(\bar{\bar{\tau}}) + \rho \vec{g} + \vec{F} \tag{2}$$

where:

ρ Fluid density (kg/m^3),
u Fluid velocity (m/s),
p Static pressure (Pa).

$\rho \vec{g}$ and $\vec{F}$ describe the gravitational body forces and external body forces (N), respectively. $\vec{F}$ is the source term representing porous media or any other model dependent source terms.

A suitable method for simulation is an essential role to obtain a reliable result for determining the proper concentration of each gas. The flow of the exhaust gas in the aluminum cell is turbulent, and the $k - \varepsilon$ model has wide application in industrial flow field and heat exchange simulation due to its wide application range, economical and reasonable precision. The standard $k - \varepsilon$ model is a semi-empirical formula, mainly depending on turbulent kinetic energy and diffusivity. The transport equations for both turbulent kinetic energy (k) and dissipation rate (ϵ) are shown in Equations (3) and (4), respectively [12].

$$\frac{\partial}{\partial t}(\rho k) + \frac{\partial}{\partial x_i}(\rho k u_i) = \frac{\partial}{\partial x_j}\left[\left(\mu + \frac{\mu_t}{\sigma_k}\right)\frac{\partial k}{\partial x_j}\right] + G_k + G_b - \rho\epsilon - Y_M + S_k \quad (3)$$

$$\frac{\partial}{\partial t}(\rho \varepsilon) + \frac{\partial}{\partial x_i}(\rho \varepsilon u_i) = \frac{\partial}{\partial x_j}\left[\left(\mu + \frac{\mu_t}{\sigma_\epsilon}\right)\frac{\partial \epsilon}{\partial x_j}\right] + C_{1\epsilon}\frac{\epsilon}{k}(G_k + C_{3\epsilon}G_b) - C_{2\epsilon}\rho\frac{\epsilon^2}{k} + S_\epsilon \quad (4)$$

where:

ρ	Density,
u_i	Velocity,
μ_t	Turbulence viscosity,
G_k and G_b	Generation of turbulence energy due to mean velocity gradient and buoyancy, respectively
Y_M	The effect of compressibility on the turbulence model which can be neglected
S_k and S_ϵ	User-defined source terms, which are taken as zero in this study
σ_ϵ and σ_k	Turbulent Prandtl numbers for k and ϵ, respectively.

The constants in the model are $\sigma_\epsilon = 1.3$; $\sigma_k = 1.0$; $C_{1\epsilon} = 1.4$; $C_{2\epsilon} = 1.9$; $C_\mu = 0.09$.

3.4 Mixing Air with Anode Gas Produced

Under the base case scenario, ambient air enters the electrolysis cell through the different slits. The purpose of introducing ambient air is to decrease the gas concentration and temperature inside the cell as well as being a consequence of limiting fugitive emissions. In this study, species transport is a suitable method for simulating the mixing of air with the gas produced at the anode, as this region contains several different gases in the gas phase.

Species transport equation shown in Eqn. (5) and Eqn. (6) is used for simulating the without reacting flow in a volumetric reaction model. It was assumed that the reaction takes place in a single phase:

$$\frac{\partial(\rho\omega_i)}{\partial t} + \nabla.(\rho\omega_i\vec{u}) = -\nabla.(\vec{J_\iota}) + R_i + S_i \quad (5)$$

$$\vec{J_\iota} = -\left(\rho D_{i,m} + \frac{\mu_t}{Sc_t}\right)\nabla\omega_i - D_{T,i}\frac{\nabla T}{T} \quad (6)$$

where:

ω_i	Mass fraction of species i participating in the reaction
$\vec{J_\iota}$	Diffusion flux of species i, generated due to the concentration gradient
$Sc_t = \frac{\mu_t}{\rho D_t}$	Turbulent Schmidt number taken as 0.7
μ_t and D_t	Turbulent viscosity and turbulent diffusivity, respectively, used in turbulent Schmidt number formulation [12].

3.5 Boundary Condition:

In this study, the boundary condition is divided into three parts. Firstly, the amount of gas produced by the anode includes CO_2 and CO gas that are produced during the electrochemical reaction. Additionally, the amount of gas produced by the anode is constant. Chemical reactions

take place near an anode assembly that result in the production of carbon monoxide and carbon dioxide. There are several elements, such as the effect of current efficiency, cell amperage and other factors that influence the rate of anode gas production. The first reaction is an electrolysis reaction where alumina is dissolved in a molten salt based on cryolite and produces aluminum and carbon dioxide. By using Faraday's Law [13], it is possible to calculate the gas anode production rate as shown in the equation (7). [14]

$$2Al_2O_3 + 3C = 4Al + 3CO_2 \quad (7)$$

Secondly, another reaction is the back reaction, when knowing the current efficiency of the cells, it is possible to stoichiometry estimate the anode gas generated from the back reaction. The reaction is shown in Eqn. (8). [14]

$$2Al + 3CO_2 = Al_2O_3 + 3CO \quad (8)$$

Then, the Boudouard reaction occurs when the CO_2 gas collides with the anode wall and produces CO gas. This reaction rate was defined using a preliminary simulation of the thermodynamic conditions in the anode cavities. The reaction is shown in Equation (9). [14]

$$CO_2 + C = 2CO \quad (9)$$

Simultaneously, part of the chemical reactions that take place between the bath and the anode can be defined by stoichiometry. These input conditions will lead to a gas flow input set as boundary conditions. Changes in amperage and current efficiency will directly affect the amount of gas produced. Secondly, the pressure on the slit surface is one atmosphere, but this pressure is not constant. During simulation, it is possible for the pressure to change at the slit surface. Thirdly, the pressure at the outlet is crucial for how the gas is distributed within the electrolysis cell. The strong fan power of the fan within the channels at the gas outlet, which causes suction, has led to local negative pressure being observed at the gas outlet. Therefore, the boundary conditions for the base case are presented in Table 1.

Table 1. Boundary conditions for the base case.

Base Case			
	Parameter	**Value**	**Unit**
Inlet	I (cell amperage)	600	kA
	Current efficiency	93	%
	Slit width	0.5	cm
Outlet	Gas Exhaust	Based on stochiometric validation	Pa

3.6 Stochiometric Validation

There are four factors that are considered to validate results from simulation. Firstly, the amount of carbon consumed, secondly the ratio of CO_2/CO, then the total amount of carbon dioxide produced and finally the total exhaust rate in normalized cubic meter per second. Every chemical reaction mentioned has an impact on carbon consumption, carbon dioxide, and the CO_2/CO ratio. The effect of various factors controlling carbon consumption is highly dependent on operational procedures. Therefore, the anode consumption during the reactions needs to be considered by adding another reaction, which is the carbon oxidation. Oxygen entering the electrolysis cells through external airflow may react with the anode to produce carbon dioxide. To achieve the targeted CO_2/CO ratio [15], which is a value of 10:1, the system is driven by stoichiometry. In reaction (7), CO_2 gas is produced, while in reactions (8) and (9), the amount of CO_2 gas is reduced

due to the production of CO gas. Finally, the required carbon oxidation is calculated in order to obtain desired ratio and the total carbon consumption is calculated to confirm that the mass balance result is close to 450 kg C/t Al [16]. The finals results are also compared to the targeted value of CO_2 concentration, which is 10 000 ppm. To validate the results, the base case model conditions were used in the validation process, and ultimately, an operational pressure of -210 Pa was defined as the recommended pressure to satisfy the validation process. The contribution of different consumption mechanisms can be summarized as shown in Table 2.

Table 2. Validation process.

Steps	Details	CO_2/CO Ratio	CO_2 concentration	Carbon consumption	Gas flowrate towards GTC
Step 1	Input conditions, amperage, and current efficiency define the CO_2 and CO emission rate.	≈ 7.60	≈ 88.15 %	≈ 357 kg C/tAl	
Step 2	Numerical simulation. Ambient air is mixed with the gas. Driven by model conditions.	No change	Reduction to ≈ 8 820 ppm	No change	Industrial value
Step 3	Stochiometric calculations. If carbon oxidation was present, how much oxidation would be necessary to reach the targeted ratio	Increase to 10	Increases to 10 700 ppm	+ 100 kg C/t Al	
Final results	For base case scenario	10	10 700 ppm	454 kg C/t Al	Industrial value
Deviation from target		N/A	+ 7 %	+ 2 %	± 4.9 %

4. Sensitivity Analysis

4.1 Experimental Plan

Multiple scenarios were designed in order to understand the expected variations on our systems coming from changes in key parameters. These changes can lead to more generation of carbon dioxide and carbon monoxide and in a few cases diminish the sum of gas created by the chemical reactions. The main purpose for this plan is to simulate a specific number of cases to illustrate the extent of operational conditions that could be foreseable in the industry.The investigated cases are shown in Table 3.

Table 3. Experimental plan.

	Parameter	Case 1	Case 2	Case 3	Case 4	Case 5	Case 6	Case 7	Case 8	Case 9
Inlet	I (cell amperage)	570	600	630	570	600	630	570	600	630
	Current efficiency	96	90	93	90	93	96	93	96	90
	Slit width	0.5	0.5	0.5	0.05	0.05	0.05	1	1	1
Outlet	Gas Exhaust	-150	-300	0	0	-150	-300	-300	0	-150

4.2 Result and Discussion

To extract valuable results for the present study, two steps are taken as follows: Firstly, the numerical results include a CO_2 concentration map in the region above the feeder hole. This contour map was used to identify the intensity of the dilution rate of CO_2 above a feeder in both extremities of the cell, thus one being at the tapping and duct end side of the cell. Secondly, the investigation of flow at the slit surface (from air inlet to the cell) allows the evaluation of the potential impact on fugitive emissions from these changes.

4.2.1 Example of These Results from the Base Case Scenario

As shown in Table 1, the CO_2 concentration map corresponds to the conditions described in the table. When air entered the electrolysis cell and mixed with the gas produced at the anode, the CO_2 concentration decreased from 881 500 ppm to 8 820 ppm. Negative pressure at the outlet sucks the gas produced at the anode and the incoming air, which enter the electrolysis cell through a slit. The incoming air, at a relatively high velocity, mixes with the gas produced at the anode, causing a drastic reduction in CO_2 concentration. In this study, the CO_2 concentration map has been investigated at the main feeders closest to the tapping and duct end of the cell, respectively. Figure 4 (tap end) and 5 (duct end) show the distribution of CO_2 concentration in the cell under two 90° directions. The tap end is placed at the end of the cell where the pressure distribution is lower, under such conditions, the gas concentration map is wider and the reduction in gas concentration is less significant than what we can observe in Figure 5.

A metric was defined to analyze the data from the numerous simulations. The area of interest was defined as the zones in the cells where the concentration of CO_2 is higher than 10 %. Then a vertical distance in meter was calculated from the feeder top surface to the most vertical point where the concentration satisfies the 10 % criteria. This value was later normalized to illustrate the fraction of the total available height that is covered by a gas concentration of CO_2 higher than 10 %. This zone is defined as the "High CO_2 concentration domain" further in the article and is presented as a relative distance. Details of the calculations are presented in Figure 4A.

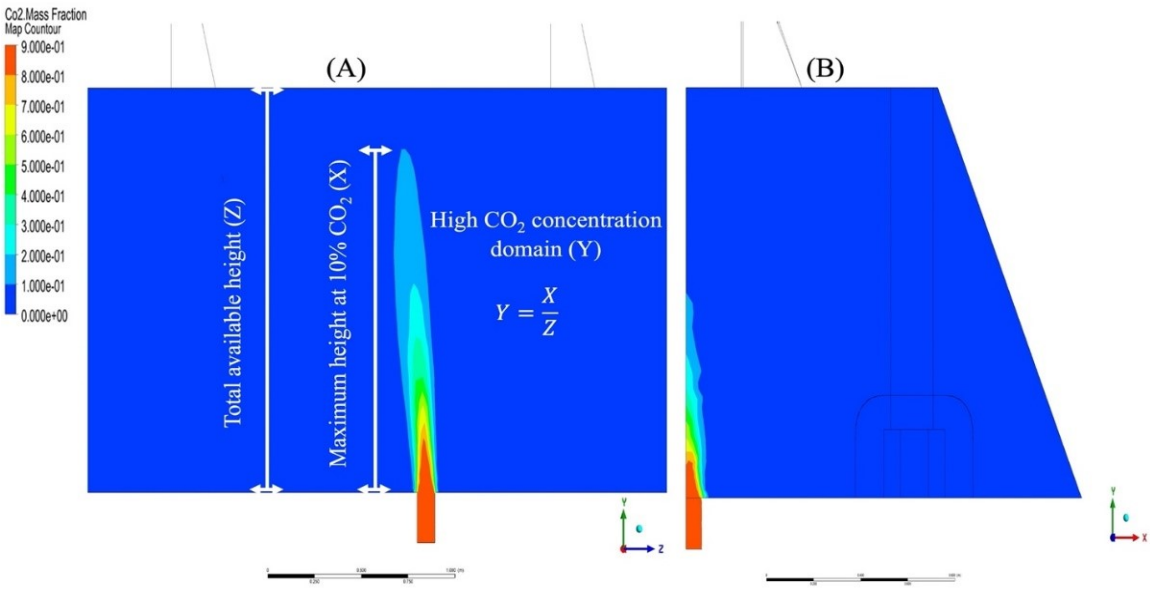

Figure 4. CO_2 mass fraction contours at the tap end for the base case. (A): front view, (B): side view.

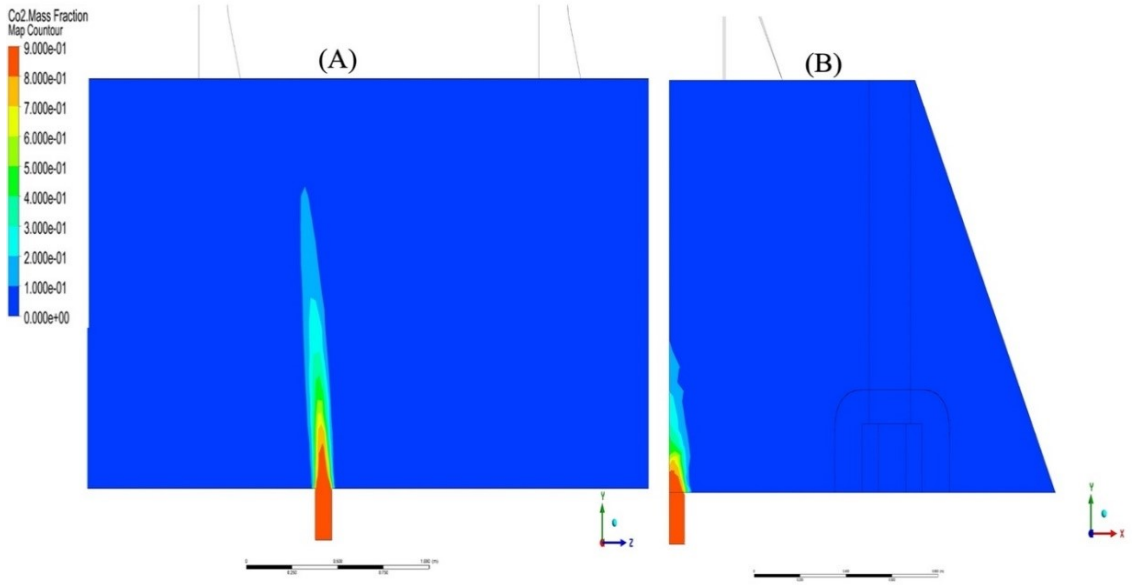

Figure 5. CO_2 mass fraction contours at the duct end for base case. Left: (A) Front view, right: (B) Side view.

4.2.2 Results from the Sensitivity Analysis

Based on the contour map presented in the previous section, it was possible to pinpoint the furthest vertical position where the CO_2 concentration reaches a concentration lower than 10 %, for each scenario investigated. Using that position, a distance was calculated as an indicator of the CO_2 dilution rate. This distance is defined as the "High CO_2 concentration domain."

As shown in Figure 6A to 6D, the changing High CO_2 concentration domain was investigated as a function of the current efficiency, current amperage, slit (gap hooding), as well as the level of negative pressure. In all but one situation, there is a small difference between the tapping and duct end of the cell, indicating that a small pressure imbalance along the length of the cell is enough to influence the CO_2 concentrations. Those spatial variations appear quite consistent throughout all the parameter change studied.

A detailed look at individual parameters indicates that an increase of the current efficiency and current amperage generates a linear increase of the High CO_2 concentration domain. This variation is logical as both these parameters essentially increase the amount of CO_2 generated at the inlet. Both these parameters are, however, very small in comparison to the effect of the other two parameters. Slit size plays a dominant role in the High CO_2 concentration domain as illustrated in Figure 6C, where an increase of the slit size will result in a consequential decrease in the High CO_2 concentration domain on all the ranged studied. According to Figure 6D, by increasing the negative pressure, the High CO_2 concentration domain will decrease in a linear behavior. As the negative pressure increases, the additional air sucked in the pot contributes to a quicker dilution of the CO_2 concentration.

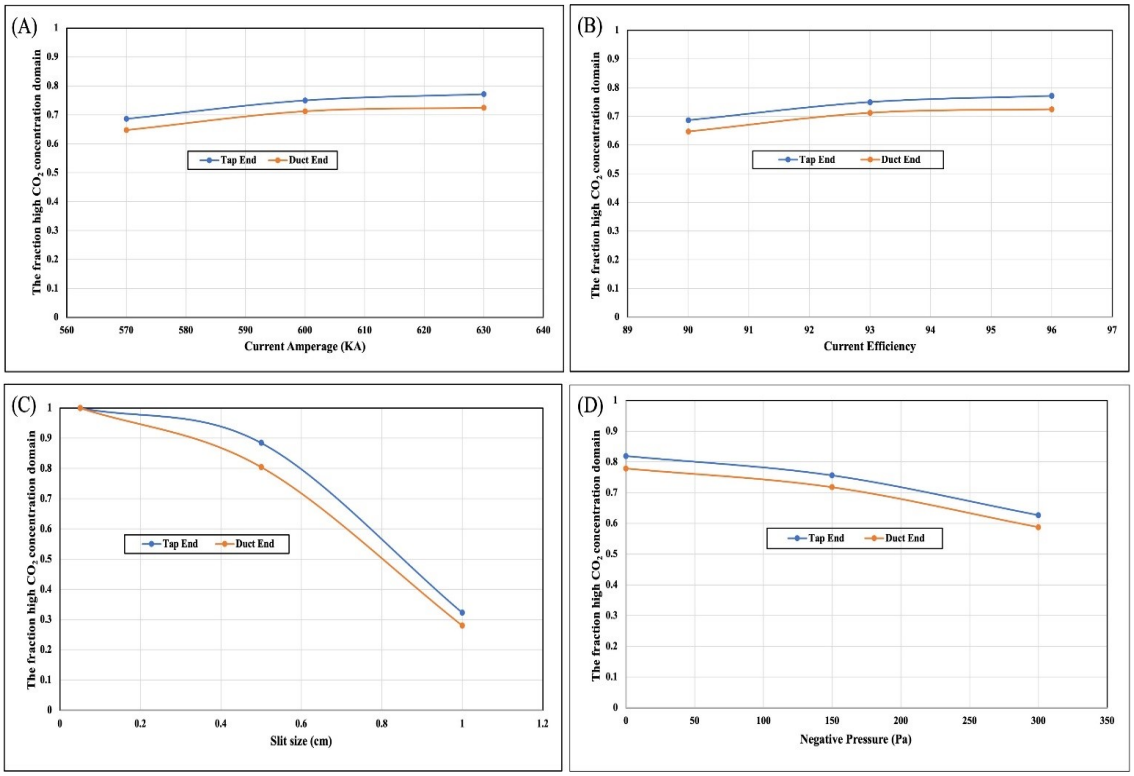

Figure 6. The trend of High CO_2 concentration domain for tap end and duct end.

4.2.3 The Changing of Fugitive Gas Emission

Figure 7 illustrates the effect of the different parameters on the rate of fugitive emission gas as a function of the position. By changing the amperage of the cell, the impact on the trend of fugitive emission, represented in Figure 7 (A), is almost minimal with variations between 2 and 6 % between regions. The effect of the current efficiency Figure 7 (B) and the effect of the slit size Figure 7 (C) is slightly more significant, with variations between 2 % and 8 % of the total emissions generated by the cells for each respective region. While these results are a bit surprising, it is important to highlight that due to the partial experience plan executed, the overall results may be sensitive to the random selection of the parameters order and have a higher uncertainty than if a full factorial design had been executed. This is particularly important in this case due to the high number of cases simulated (66 % of scenarios) where the fugitive emissions were negligible, thus equal to zero. Therefore, the effect of the cases with an exhaust pressure of 0 Pa outweigh the results of other scenarios and explain the strange effect observed from the effect of amperage, current efficiency and slit size. Unfortunately, an expansion of the experimental design will be necessary in order to properly define the realistic effect of these three parameters on the total risk of fugitive emissions. Finally, in Figure 7 (D), the results indicate that increasing the negative pressure significantly contributes to the decrease in the fugitive emission gas. However, increasing the negative pressure between (-150 Pa and -300 Pa) has no effect on the trend of fugitive emission gas on cell.

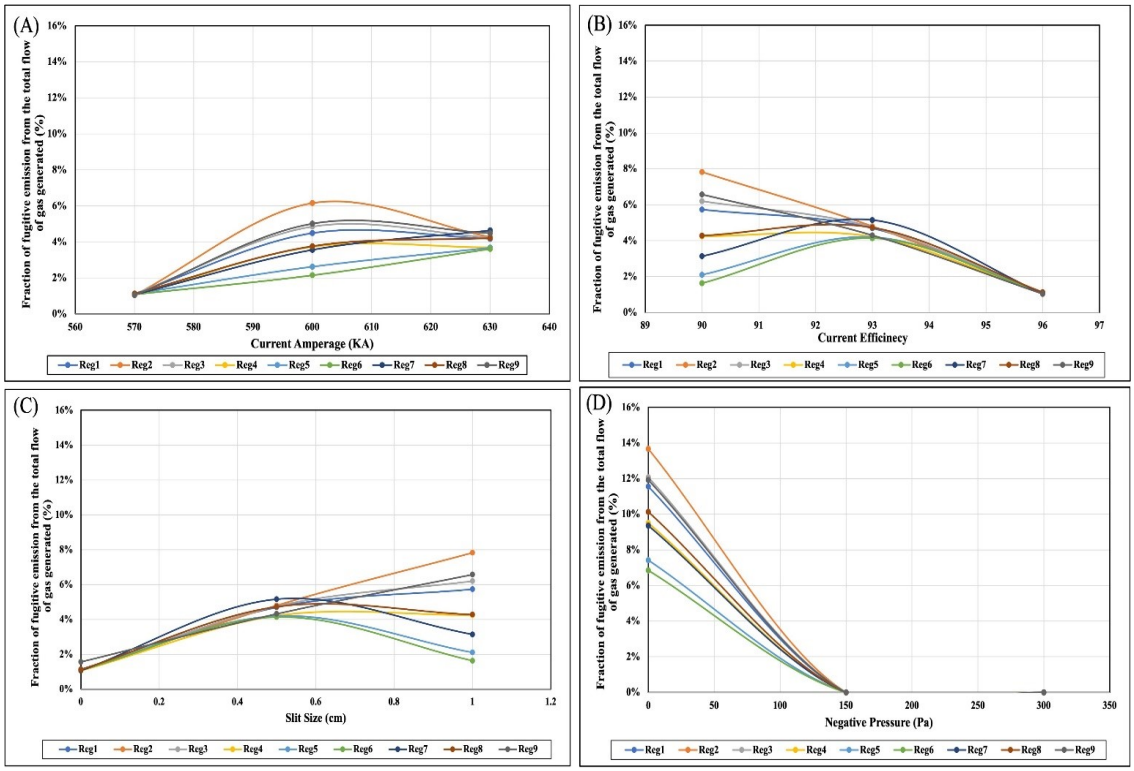

Figure 7. The trend of fugitive emission gas on cell for 9 regions.

5. Conclusions

In order to investigate the influence of negative pressure on gas exhaust, the size of the slit, cell amperage, and current efficiency on CO_2 concentration in an electrolysis cell, numerical methods have been employed. This model solves the continuity equation, the Navier-Stokes equation; the species transport equation, and the turbulence equation to determine the flow field and species distributions within the system. Our main findings can be summarized as follows.

This project will advance the progress in identifying the CO_2 concentration range under a wide range of operational conditions. It aims to specify the gas concentration at the feeder holes and define optimized conditions where CO_2 could be extracted and redirected to carbon sequestration to reduce global greenhouse gas emissions. While the study investigated the effect of cell amperage and current efficiency, the effect of these parameters is minimal on the overall pathway to overcome the challenges present for the industry.
In this study, we could confirm that increasing the negative pressure at the gas exhaust resulted in more air entering the cell, leading to a more rapid dilution of the CO_2. More importantly, changing the slit size significantly influenced the CO_2 concentration above the feeder holes. These results will pave the way for the next phase of our work in order to investigate innovative approach to control the CO_2 concentration by exploring typical and atypical ways to minimize the air infiltration coming from cell hooding during standard cell operations.

While the effect of the exhaust's negative pressure plays a significant role in the distribution of fugitive emissions, it was impossible to confirm the exact behavior of the other parameters at this point, but their effect appears to be less significant than the exhaust pressure. While the general behavior of the indicators investigated were anticipated, the study offers insight on the magnitude of their respective influence over the CO_2 concentration in opposition to the increased risk of fugitive emissions. Therefore, it is possible to pinpoint, with additional simulations, the optimal

range of cell conditions that could favor a reduced CO_2 dilution rate while limiting the risk of fugitive emissions.

Finally, this work also highlighted that the base case operational scenario is likely much stronger than needed to prevent fugitive emissions under idealistic hooding conditions. While the real operations scenarios need to be taken into consideration, along with expected cell operations that will influence the opening of the hoods and tapping door. A periodic modulation of the exhaust pressure quickly appears as a suitable potential solution that could increase the CO_2 concentration in specific local regions of the electrolysis cell.

Future developments using this model will require thorough experimental in-situ validations in order to provide even more precise investigations regarding concrete or futuristic solutions to reduce the dilution rate of the carbon dioxide while mitigating the potential harm coming from fugitive emissions.

6. Acknowledgements

The authors express their gratitude to Rio Tinto for their technical collaboration, the financial support and the permission to publish these results. The authors would also like to thank the Natural Sciences and Engineering Research council of Canada (NSERC) and the Regroupement Aluminum (REGAL) for their financial support.

7. References

1. André Charette, Yasar S. Koçaefe, and Duygu Koçaefe, Le carbone dans l'industrie de l'aluminium, 2012 Les presses de l'aluminium.
2. Richard McDonough, Aluminum Industry in Canada, *Aluminum International Today*, November-December 2022, 33-37.
3. Olivier Jos, Peters Jeroen, and Greet Maenhout, *Trends in global CO_2 emissions,* 2012 report, European Commission, PBL Netherlands Environmental Assessment Agency.
4. Udara S. P. R. Arachchige, Dinesh Kawan, and Morten C. Melaaen, Simulation of carbon dioxide capture for aluminum production process, *International Journal of Modeling and Optimization*, 2014, 43-50.
5. Philippe Ouzilleau, Aimen E. Gheribi, and Patrice Chartrand, Prediction of CO_2/CO formation from the (primary) anode process in aluminum electrolysis using an electro thermodynamic model (for coke crystallites), *Electrochimica Acta*, 2018, 916-929.
6. Mengzhi Guo et al., A highly efficient and stable composite of polyacrylate and metal–organic framework prepared by interface engineering for direct air capture, *ACS Appl. Mater. Interfaces* 2021, 13, 18, 21775–21785.
7. Sithara Dayarathna et al., Simulation of CO_2 capture from an aluminum production plant, *WIT Transactions on Ecology and the Environment*, 2014, 729-739.
8. Annete Mathisen et al., Investigation into optimal CO_2 concentration for CO_2 capture from aluminum production, *Energy Procedia*, Volume 37, 2013, 7168-7175.
9. Hongliang Zhang et al., Numerical Simulation Study on Gas Collecting System of 400 kA Grade Aluminum Electrolytic Cell, *Light Metals* 2018, 573-586.
10. LI Xue-jiao et al, Numerical Simulation Study on Gas Gathering Structure of Aluminum Reduction Cell, *Journal of Northeastern University (Natural Science)*, 2022, 43 pages.
11. Odd Edgar Bjarno, and Geir Wedde, A device and a method of cleaning an effluent gas from an aluminum production electrolytic cell, Canadian Patent Application CA 2 827 357C, Publication date 2012/08/23.
12. *ANSYS FLUENT Theory Guide,* ANSYS 2011, 794 pages.
13. P. Fellner et al., *Aluminum Electrolysis: Fundamentals of the Hall-Héroult Process,* Beuth Verlag GmbH, 2011.

14. Asbjorn Solheim, and amuel Senanu, Recycling of the flue gas from aluminum electrolysis cells, *Light Metals* 2020, 803-810.
15. Thor Anders Aarhaug, and Arne Petter Ratvik, Aluminum primary production off-gas composition and emissions, *JOM*, February 2019, Vol. 71, 2966-2977, https://doi.org/10.1007/s11837-019-03370-6.
16. Kai Grjotheim, and Halvor Kvande, *Introduction to Aluminum Electrolysis,* Aluminum-Verlag 1993, Düsseldorf, Germany, 260 pages.